www.ijecs.in
International Journal Of Engineering And Computer Science ISSN:2319-7242
Volume – 5 Issue -02 February, 2016 Page No. 15787-15800

Convective heat transfer in Water Functionalized Carbon Nanotube Flow past a Static/Moving wedge with heat source/sink

G.Venkataramanaiah[1], Dr.M.Sreedhar Babu[2], M.Lavanya[3]

[1]Research scholar,
Dept. of Applied Mathematics,
Yogi Vemana University, Kadapa
Andhra Pradesh, India.
Email: gorla.venkataramanaiah@gmail.com,
Cell no: 9885229604.

[2]Asst.professor,
Dept. of Applied Mathematics,
Yogi Vemana University, Kadapa
Andhra Pradesh, India.
Email: msreedharyvu@gmail.com,
Cell no: 9959656072.

[3]M.Lavanya
Research scholar,
Dept. of Applied Mathematics,
Yogi Vemana University, Kadapa
Andhra Pradesh, India.
Email: lavanya786mamidi@gmail.com,
Cell no: 9494218601.

ABSTRACT

The MHD flow and convective heat transfer from water functionalized CNTs over a static/moving wedge in the presence of heat source/sing are studied numerically. Thermal conductivity and viscosity of both single and multiple wall carbon nanotubes (CNTs) within a base fluid (water) of similar volume are investigated to determine the impact of these properties on thermo fluid performance. The governing partial differential equations are converted into nonlinear, ordinary, and coupled differential equations and are solved using bvp4c Matlab solver. The effects of volume fraction of CNTs and magnetic and wedge parameters are investigated and presented graphically. The numerical results are compared with the published data and are found to be in good agreement.

Keywords: MHD, Nanotube, Heat Transfer, Viscous Dissipation, Heat Source/Sink, Convective Boundary Condition.

1. Introduction

Nanoparticles have one dimension that measures 100 nanometers or less. The properties of a lot of conventional materials change when formed from nanoparticles. This is typically to because nanoparticles contain a greater surface area per weight than larger particles which cause them to be more reactive to some other molecules. Choi [1] investigated the theoretical of the thermal conductivity of nanofluids with Copper nanophase materials and he estimated the potential gain of the fluids and also he showed that one of the benefits of nanofluids will be dramatic reductions in heat exchanger pumping power. The characteristic feature of nanofluids is thermal conductivity enhancement, a phenomenon observed by Masuda et al. [2]. This phenomenon suggests the opportunity of using nanofluids in advanced nuclear systems [3]. A comprehensive survey of convective transport in nanofluids was made by Buongiorno [4], who says that a satisfactory explanation for the abnormal increase of the thermal conductivity and viscosity is yet to be found. He focused on added heat transfer enhancement observed in convective situations. Kuznetsov and Nield [5] have examined the influence of nanoparticles on natural convection boundary-layer flow over a vertical plate using a model in which Brownian motion and thermophoresis are accounted for. The authors have assumed the simplest possible boundary conditions, namely those in which both the temperature and the nanoparticle fraction are constant along the wall. Furthermore, Nield and Kuznetsov [6, 7] have studied the Cheng and Minkowycz [8] problem of natural convection over a vertical plate in a porous medium saturated by a nanofluid and used the nanofluid incorporates for the effects of Brownian motion and thermophoresis for the porous medium.

Carbon nanotubes (CNTs), due to cylindrical carbon molecules origin, are found to have special thermal properties with very high thermal conductivities. The diameter of CNTs ranges from 1 to 100 nm and has lengths in micrometer. The thermal conductivity of single-wall CNT up to 6,600 W/m K and for multi-wall CNT up to 3,000 W/m K has been reported in Hone [9] and Antar et al. [10].

Ding et al. [11] investigated the heat transfer behavior of CNT nanofluids flowing through a horizontal tube. They observed significant enhancement of the convective heat transfer and found that the enhancement depends on the Reynolds number and solid volume fraction of CNTs. Kamali and Binesh [12] numerically investigated the convective heat transfer of multi-wall carbon nanotube (MWCNT)-based nanofluids in a straight tube under constant wall heat flux condition. They solved Navier Stokes equations using the finite volume technique considering CNT-based nanofluids using power law model. They found that the heat transfer coefficient is dominated by the wall region due to non-Newtonian behaviour of CNT nanofluid. Meyer et al. [13] investigated experimentally the convective heat transfer enhancement of aqueous suspensions of multi-walled CNTs flowing through astraight horizontal tube. They determined the heat transfer coefficients and friction factors as a function of Reynolds number. They found that heat transfer was enhanced when comparing the data on a Reynolds Nusselt graph and the increase in viscosity was four times the increase in the thermal conductivity. Khan et al. [14] investigated the fluid flow and heat transfer of carbon nanotubes along a flat plate with Navier slip boundary and concluded that the skin friction and heat transfer rates increase with CNT volume fraction. Khan et al. [15] investigated the MHD flow and heat transfer from water functionalized CNTs over a static/moving wedge and also concluded that the magnetic field reduces boundary layer thickness and increases skin friction and Nusselt numbers.

Viscous dissipation effects are usually ignored in macro scale systems, in laminar flow in particular, except for very viscous liquids at comparatively high velocities. However, even for common liquids at laminar Reynolds numbers, frictional effects in micro scale systems may change the energy equation [16]. Koo and Kleinstreuer [17] have investigated the effects of viscous dissipation on the temperature field using dimensional analysis and experimentally validated computer simulations. Three common working fluids-water, methanol and *iso*-propanol-in different conduit geometries have been considered in this study. The authors concluded that the channel size was a key factor that determines the impact of viscous dissipation. Furthermore, viscous dissipation effects may be very significant for fluids with high viscosities and low specific heat capacities, even at relatively low Reynolds numbers. Accordingly, the viscous dissipation term should be considered in the micro scale systems. Yazdi et al. [18] evaluated the slip MHD flow and heat transfer of an electrically conducting liquid over a permeable surface in the presence of the viscous dissipation effects under convective boundary conditions. Khan et al. [19] studied the Unsteady MHD free convection boundary-layer flow of a nanofluid along a stretching sheet with thermal radiation and viscous dissipation effects using finite difference method. Khan et al. [20] studied the viscoelastic MHD flow, heat and mass transfer over a porous stretching sheet with dissipation of energy and stress work. Makinde [21] concluded that the heat transfer rate at the moving plate surface increases with the increases in the nanoparticle volume fraction (φ) and the Biot number (*Bi*), while it decreases with the increase in the Brinkmann number (Br) due to viscous heating. Chandrasekar and Baskaran [22] studied the thermo dynamical modelling of viscous dissipation in magnetohydrodynamic Flow. Hady et al. [23] concluded that an increment in the solid volume fraction and the Eckert number yields an increment in the nanofluid's temperature; this leads to a rapid reduction in the heat transfer rates.

However, the interactions of the MHD flow and heat transfer from water functionalized CNTs over a static/moving wedge in the presence of heat source/sing and convective boundary condition. The governing boundary layer equations have been transformed to a two-point boundary value problem in similarity variables and the resultant problem is solved numerically using bvp4c MATLAB solver. The effects of various governing parameters on the fluid velocity, temperature, Skin-friction and the rate of heat transfer are shown in figures and analyzed in detail.

2. Mathematical Formulation

Consider steady two-dimensional boundary layer flow past a static or a moving wedge in a water-based nanofluid containing SWCNTs and MWCNTs. Geometry of the problem is shown in figure A.

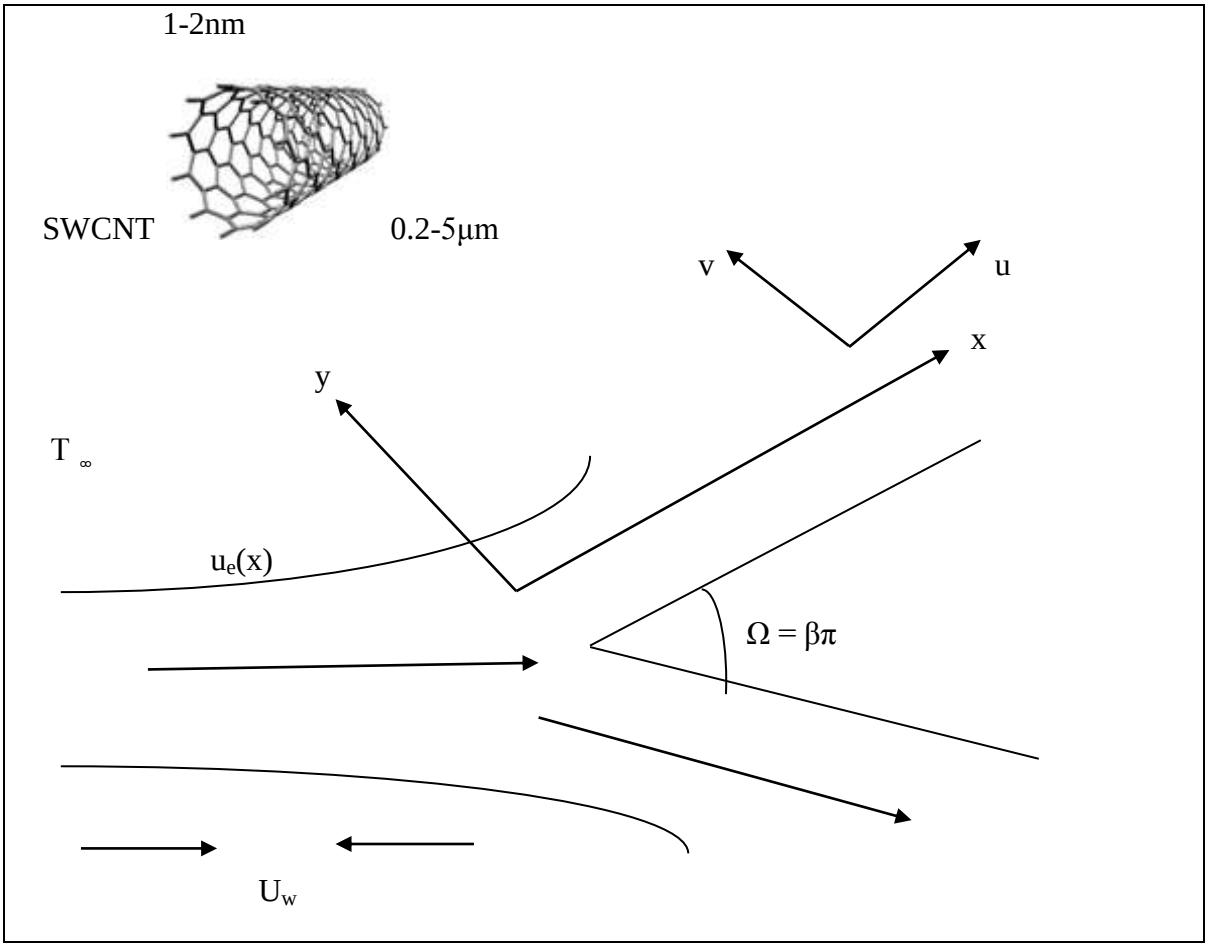

(a)

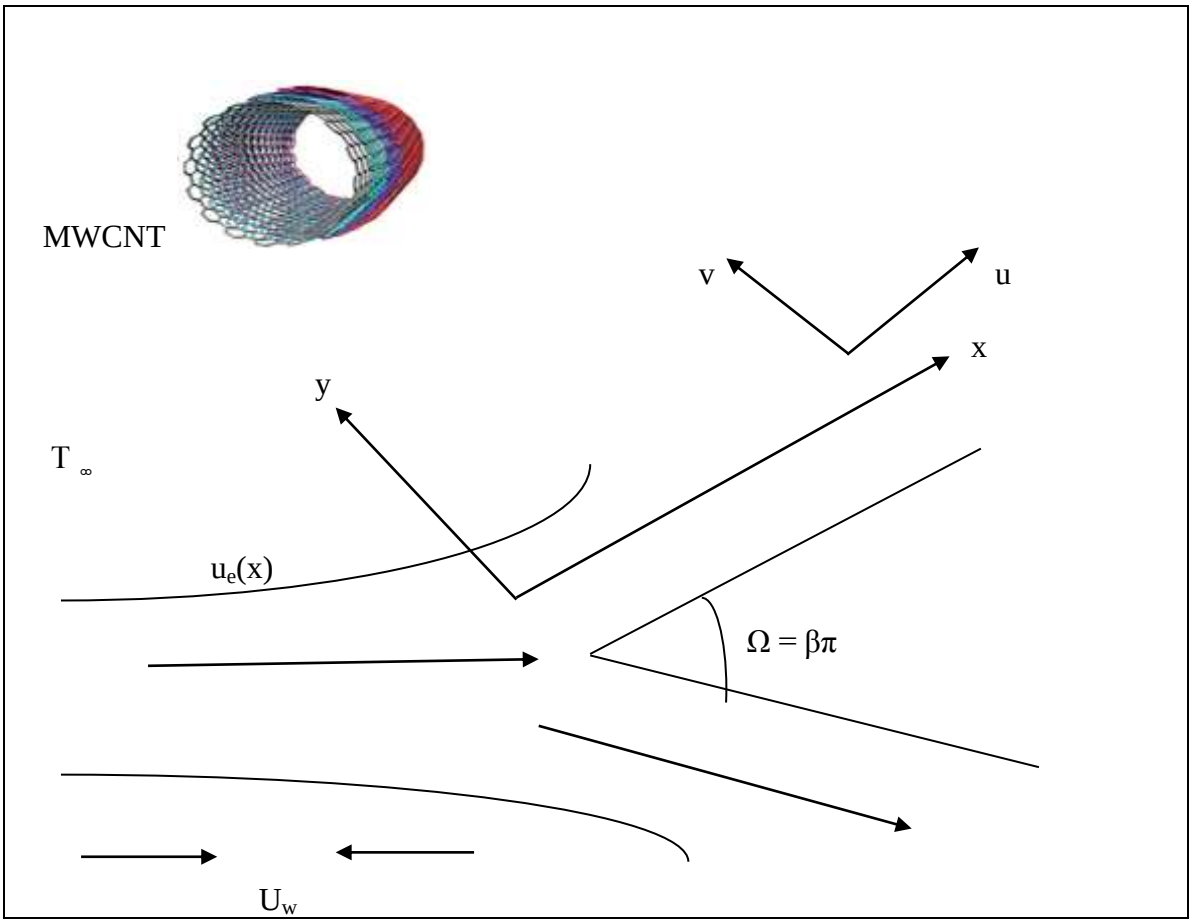

(b)

Figure A: Geometry of the Problem

The nanofluid is assumed incompressible and the flow is assumed to be steady and laminar. It is also assumed that the base fluid (i.e., water) and the nanoparticles are in thermal equilibrium and no slip occurs between them. The thermophysical properties of the fluid and nanoparticles are given in Table 1.

Table 1: Thermophysical properties of water and CNTs [24, 25]

Thermophysical properties	Base fluid Water	Carbon nanotubes	
		SWCNT	MWCNT
ρ (kg/m^3)	997	2600	1600
c_p (J/kg-K)	4179	425	796
k (W/m-K)	0.613	6600	3000
Pr	6.2	---	

Further, it is assumed that the velocity of the free stream (in viscid flow) is $u_e(x) = U_\infty x^m$ and that of the moving wedge is $u_w(x) = U_w x^m$, where U_∞, U_w and m are constants with $0 \le m \le 1$. We consider a two-dimensional Cartesian coordinate system (x, y), where x and y are the coordinates measured along the surface of the wedge and normal to it, respectively. Under the boundary layer approximations, the basic steady conservation of mass, momentum, and energy equations can be written as

Continuity equation

$$\frac{\partial u}{\partial x} + \frac{\partial v}{\partial y} = 0 \qquad (2.1)$$

Momentum equation

$$u\frac{\partial u}{\partial x} + v\frac{\partial u}{\partial y} = U_e\frac{dU_e}{dx} + \nu_{nf}\frac{\partial^2 u}{\partial y^2} - \frac{\sigma B_0^2}{\rho_{nf}}(U_e - u) \qquad (2.2)$$

Energy equation

$$u\frac{\partial T}{\partial x} + v\frac{\partial T}{\partial y} = \alpha_{nf}\frac{\partial^2 T}{\partial y^2} - \frac{1}{\rho c_p}\frac{\partial q_r}{\partial y} + \frac{\nu_{nf}}{(\rho c_p)_{nf}}\left(\frac{\partial u}{\partial y}\right)^2 + \frac{Q_0}{(\rho c_p)_f}(T - T_\infty) \qquad (2.3)$$

The boundary conditions are

$$u = u_w(x), v = 0, -k\frac{\partial T}{\partial y} = h_f(T_w - T) \quad \text{at} \quad y = 0$$
$$u \to u_e(x), T \to T_\infty \quad \text{as} \quad y \to \infty \qquad (2.4)$$

Here u and v are the velocity components along the x- and y- axes, respectively. T is the temperature of the base fluid, Q_0 is the heat source/sink constant, h_f is the convective heat transfer coefficient, ν_{nf} is viscosity of the nanofluid, ρ_{nf} is the density of the nanofluid, and α_{nf} is the thermal diffusivity of nanofluid, which are given by

$$\nu_{nf} = \frac{\mu_{nf}}{\rho_{nf}}, \mu_{nf} = \frac{\mu_f}{(1-\phi)^{2.5}}, \alpha_{nf} = \frac{k_{nf}}{\rho_{nf}(C_p)_{nf}}, \rho_{nf} = (1-\phi)\rho_f + \phi\rho_{CNT}$$
$$(\rho C_p)_{nf} = (1-\phi)(\rho C_p)_f + \phi(\rho C_p)_{CNT} \qquad (2.5)$$
$$\frac{k_{nf}}{k_f} = \left(1 - \phi + 2\phi\frac{k_{CNT}}{k_{CNT} - k_f}\ln\frac{k_{CNT} + k_f}{2k_f}\right)\left(1 - \phi + 2\phi\frac{k_f}{k_{CNT} - k_f}\ln\frac{k_{CNT} + k_f}{2k_f}\right)^{-1}$$

where μ_f is the viscosity of base fluid, ϕ is the nanoparticle fraction, $(\rho Cp)_{nf}$ is the effective heat capacity of CNTs, $k$nf is the thermal conductivity of nanofluid, k_f and k_{CNT} are the thermal conductivities of the base fluid and CNTs, respectively, and ρ_f

and ρ_{CNT} are the thermal conductivities of the base fluid and CNTs, respectively. Introducing the following similarity transformations,

$$\psi = \left[\frac{2\nu_f x u_e(x)}{m+1}\right]^{1/2} f(\eta), \theta(\eta) = \frac{T-T_\infty}{T_w-T_\infty}, \eta = \left[\frac{(m+1)u_e(x)}{2\nu_f x}\right]^{1/2} y \qquad (2.6)$$

where ψ is the stream function and is defined in the usual way as $u = \partial\psi/\partial y$ and v = $-\partial\psi/\partial x$ so as to identically satisfy (2.1) and ν_f is the kinematic viscosity of the base fluid. On substituting (2.6) into (2.2) and (2.3) along with the boundary conditions defined in (2.4), we obtain the following ordinary differential equations:

$$\frac{1}{(1-\phi)^{2.5}\left(1-\phi+\phi\rho_{CNT}/\rho_f\right)} f''' + ff'' + \left(\frac{2m}{m+1}\right)\left(1-f'^2\right) + \frac{M^2}{\left(1-\phi+\phi\rho_{CNT}/\rho_f\right)}\left(1-f'^2\right) = 0 \qquad (2.7)$$

$$\frac{1}{\Pr}\left(\frac{k_{nf}/k_f}{\left(1-\phi+\phi\left(\rho c_p\right)_{CNT}/\left(\rho c_p\right)_f\right)}\right)\theta'' + f\theta' + \frac{Ec}{(1-\phi)^{2.5}} f''^2 + Q\theta = 0 \qquad (2.9)$$

The transformed boundary conditions can be written as

$$f(0) = 0,\ f'(0) = S,\ \theta'(0) = -Bi\left[1-\theta(0)\right]$$
$$f' \to 1, \theta \to 0 \quad \text{as} \quad \eta \to \infty \qquad (2.10)$$

where primes denote differentiation with respect to η

The physical quantities of interest are the wall skin friction coefficient C_f, and the local Nusselt number Nu_x which are defined as

$$C_f = \frac{\tau_w}{\rho_f u_e^2}, Nu_x = \frac{x q_w}{k_f\left(T_w - T_\infty\right)} \qquad (2.11)$$

where τ_w is the shear stress, and q_w is the heat flux from the sheet are defined as

$$\tau_w = \mu_{nf}\left(\frac{\partial u}{\partial y}\right)_{y=0}$$
$$q_w = -k_{nf}\left(\frac{\partial T}{\partial y}\right)_{y=0} \qquad (2.12)$$

Thus, we get the wall skin friction coefficient C_{fx}, the local Nusselt number Nu_x and the local Shear wood number Sh_x as follows:

$$C_f \,\mathrm{Re}_x^{\frac{1}{2}} = \sqrt{\frac{m+1}{2}}\frac{1}{(1-\phi)^{2.5}} f''(0)$$
$$\mathrm{Re}_x^{\frac{-1}{2}} Nu_x = -\sqrt{\frac{m+1}{2}}\frac{k_{nf}}{k_f}\theta'(0) \qquad (2.13)$$

where $\mathrm{Re}_x = \frac{u_e x}{\nu_f}$ is the local Reynolds number.

3 Solution Of The Problem

The set of equations (2.7) to (2.9) were reduced to a system of first-order differential equations and solved using a MATLAB boundary value problem solver called **bvp4c**. This program solves boundary value problems for ordinary differential equations of the form $y' = f(x, y, p), a \le x \le b$, by implementing a collocation method subject to general nonlinear, two-point boundary conditions $g\left(y(a), y(b), p\right)$. Here ***p*** is a vector of unknown parameters. Boundary value problems (BVPs) arise in most diverse forms. Just about any BVP can be formulated for solution with **bvp4c**. The first step is to write the *ODEs* as a system of first order ordinary differential equations. The details of the solution method are presented in Shampine and Kierzenka[26].

4 Results And Discussion

MHD flow of water-based carbon nanotubes (CNTs) over static and moving wedges with viscoud dissipation in the presence of convective boundary condition and heat source/sink is investigated numerically. The thermophysical properties of water and both CNTs are presented in Table 1. The numerical results are compared in Tables 2 and 3 for skin friction and in Tables 4 and 5 for heat transfer in some special cases. The results are found to be in excellent agreement with the published data. The effects of the magnetic field and volume fraction of

SWCNTs on the dimensionless velocity are displayed in Figures 2 and 3 for flow past horizontal and near the stagnation point of vertical stationary and moving flat plates, respectively. It can be seen that the hydrodynamic boundary layer thickness is larger in the absence of a magnetic field in each case. In fact, the magnetic field tends to reduce the boundary layer thickness. Figures 1(a) and 1(b) depict velocity profiles for the flow of SWCNTs over a stationary horizontal plate (m = 0) and near the stagnation point of a vertical stationary plate (m = 1), respectively. In the absence of magnetic field, the effect of volume fraction of SWCNTs on the dimensionless velocity can be noticed but as the magnetic field increases, its effect diminishes. When the horizontal and vertical plates move in the free stream direction, the dimensionless velocity profiles are shown in Figures 2(a) and 2(b), respectively. It is important to note that the boundary layer thickness is reduced in this case. The effects of volume fraction of CNTs are found to be negligible and the velocity boundary layer thickness reduces with an increase in magnetic field in both cases.

The effects of magnetic field and volume fraction of SWCNTs on temperature are illustrated in Figure 3(a) for flow past horizontal plate (m=0) fig 3(b) for flow near a stagnation point of vertical flat plate (m=1) respectively. In each case, the magnetic field tends to reduce the thermal boundary layer thickness. The comparison of Figures 4(a) and 4(b) shows that the thermal boundary layer thickness is smaller in the case of flow over a horizontal plate and hence less thermal resistance is offered in this case. However, when the plates are moving in the direction of the free stream, the magnetic field has no appreciable effect on the thermal boundary layer thickness (as shown in Figures 4(a) and 4(b)). Conventional fluids (ϕ = 0) have a smaller thermal boundary layer thickness and as the volume fraction of SWCNTs increases, the thermal boundary layer thickness also increases due to an increase in the density of CNTs.

Figures 5(a) and 5(b) depict $\theta(\eta)$ on Eckert number and convective parameter for the flow of SWCNTs over a stationary horizontal plate (m = 0) and near the stagnation point of a vertical stationary plate (m = 1), respectively. Temperature of the fluid increases with the influence of Ec but decrease with Bi. Figures 6(a) and 6(b) depict $\theta(\eta)$ on heat source/sink and wedge parameter for the flow of SWCNTs over a stationary horizontal plate (m = 0) and near the stagnation point of a vertical stationary plate (m = 1), respectively. Temperature of the fluid increases with the influence of Q but decrease with S.

The variation of skin friction with magnetic field and volume fraction of CNTs is presented in Figure 7 for the horizontal plate moving in an opposite direction to the free stream. In Figure 7(a), SWCNTs are used whereas in Figure 7(b) MWCNTs are used to show the comparison of skin friction in the presence of a magnetic field. It is noticed that the skin friction increases with volume fraction of CNTs in both cases. However, skin friction of SWCNTs is found to be higher than MWCNTs. It is due to higher density of SWCNTs than MWCNTs (Table 1). The effect of magnetic field creates a Lorentz force which acts against the flow and thus enhances the skin friction. As the horizontal plate moves in the opposing flow, the hydraulic resistance also increases which helps in an increase in skin friction. When the horizontal plate moves in an assisting flow, Figures 8(a) and 8(b) show the variation of skin friction with volume fraction of CNTs and magnetic field. In this case, the resistance decreases and hence the skin friction decreases with an increase in the plate velocity. The same behavior was observed when a vertical plate moves in opposing flow.

Figures 9(a) and 9(b) present the variation of skin friction of CNTs along vertical plate moving in opposite direction to the free stream in the presence of a magnetic field. Due to the increase in density with volume fraction of CNTs, the skin friction increases with volume friction of CNTs and magnetic parameter. Figures 10(a) and 10(b) present the variation of skin friction of CNTs along vertical plate moving in same direction to the free stream in the presence of a magnetic field. Due to the increase in density with volume fraction of CNTs, the skin friction increases with volume friction of CNTs and magnetic parameter.

The variation of Nusselt numbers with volume fraction of CNTs, magnetic and volume fraction is reported in Figures 11–14 for special cases. Due to higher thermal conductivity, SWCNTs possess higher Nusselt numbers in each case. The effects of magnetic field and the motion of the horizontal plate in the direction opposite to the free stream are shown in Figure 11(a) for SWCNTs and in Figure 11(b) for MWCNTs. It is noticed that Nusselt numbers decrease with an increase in the plate velocity. However, magnetic field helps in increasing Nusselt numbers for both CNTs. The same behavior can be observed in Figure 12 for a vertical plate and in Figure 12 for a wedge moving in opposite direction to the free stream. However, when the horizontal plate moves in the direction of free stream, the Nusselt numbers increase with plate velocity. This is shown in Figure 13(a) for SWCNTs and in Figure 13(b) for MWCNTs. The same behavior can be observed in Figure 14 for a vertical plate.

The variation of Nusselt numbers with convective parameter of CNTs, heat source/sink parameter and volume Eckert number is reported in Figures 15–16 for special cases. The effects of heat source/sink and the viscous dissipation of the horizontal plate in the direction of the free stream are shown in Figure 15(a) for SWCNTs and in Figure 15(b) for MWCNTs. It is noticed that Nusselt numbers decrease with an increase in the Q and Ec. However, convective parameter helps in increasing Nusselt numbers for both CNTs. The same behavior can be observed in Figure 16 for a vertical plate and in Figure 16 for a wedge moving in direction of the free stream.

5 Conclusions

In this paper the MHD flow and heat transfer from water functionalized CNTs over a static/moving wedge in the presence of heat source/sing and convective boundary condition are studied. Using similarity transformations, the governing equations are transformed to self-similar ordinary differential equations which are then solved using Bvp4c MATLAB solver. From the study, the following remarks can be summarized.

1. A magnetic field increases skin friction and heat transfer rates.

2. Convective parameter increases the heat transfer rate but decreases the temperature of the fluid.
3. Heat source/sink and viscous dissipation decreases the heat transfer rates but increases the temperature of the fluid.
4. Velocity boundary layer thickness is smaller for the flow near the stagnation point of vertical stationary/moving flat plates.
5. Thermal boundary layer thickness is smaller for the flow past horizontal stationary/moving flat plates.
6. MWCNTs offer less friction in each case.
7. Heat transfer rates increase when plates move in the free stream direction.
8. Heat transfer rates decrease when plates move in opposite direction to the free stream.

Table 2: Comparison of skin friction $f''(0)$ when M = S = Ec = Bi = Q = 0 for a conventional fluid (ϕ = 0).

m	$f''(0)$					
	Present Study	White [27]	Yacob et al. [28]	Yih [29]	Khan and Pop [30]	Khan et al. [15]
0	0.4696	0.4696	0.4696	0.4696	0.4696	0.4696
1/11	0.6550	0.6550	0.6550	0.6550	0.6550	0.6550
1/5	0.8021	0.8021	0.8021	0.8021	0.8021	0.8021
1/3	0.9277	0.9277	0.9277	0.9276	0.9277	0.9277
½	1.0389	1.0389	1.0389	---	1.0389	1.0389
1	1.2326	1.2326	1.2326	1.2326	1.2326	1.2326

Table 3: Comparison of skin friction $f''(0)$ when M = S = Ec = Bi = Q = 0 for a conventional fluid (ϕ = 0).

β	$f''(0)$			
	Present study	Kuo [31]	Rajagopaletal.[32]	Khan et al. [15]
0.05	0.4696	0.4696	0.4696	0.4696
0.1	0.5311	0.5317	0.5311	0.5311
0.1	0.5870	0.5879	0.5870	0.5870
0.2	0.6867	0.6876	0.6867	0.6867
0.3	0.7748	0.7755	0.7748	0.7748
0.4	0.8544	0.8549	0.8544	0.8544
0.5	0.9277	0.9279	0.9277	0.9277
0.6	0.9958	0.9958	0.9958	0.9958
0.7	1.0598	1.0594	---	1.0598
0.8	1.1203	1.1196	1.1203	1.1203
0.9	1.1777	1.1767	---	1.1777
1	1.2326	1.2313	1.2326	1.2326
2	1.6872	1.6831	---	1.6872

Table 4: Comparison of dimensionless heat transfer $-\theta'(0)$ when M = S = Ec = Bi = Q = 0 for a conventional fluid (ϕ = 0).

m	$-\theta'(0)$				
	Present study	Kuo [31]	Blasius[33]	Khan and Pop[30]	Khan et al. [15]
0	0.8769	0.8673	0.8673	0.8769	0.8769
1	1.1280	1.1147	1.1152	1.1279	1.1280

DOI: 10.18535/ijecs/v5i2.22

Table 5: Comparison of dimensionless heat transfer $-\theta'(0)$ when M = S = Ec = Bi = Q = 0 for a conventional fluid (ϕ = 0).

Pr	$-\theta'(0)$											
	B=0				B=0.3				B=1			
	Present study	White [27]	Kuo [31]	Khan et al. [15]	Present study	White [27]	Kuo [31]	Khan et al.	Present study	White [27]	Kuo [31]	Khan et al. [15]
1	0.4696	0.4696	0.4696	0.4696	0.5195	0.5195	0.5200	0.5195	0.5705	0.5705	0.5708	0.5705
2	0.5972	0.5972	0.5972	0.5972	0.6690	0.6691	0.6696	0.6690	0.7437	0.7437	0.7441	0.7437
3	0.6860	0.6860	0.6860	0.6860	0.7734	0.7734	0.7741	0.7734	0.8652	0.8652	0.8657	0.8652
6	0.8673	0.8673	0.8673	0.8673	0.9873	0.9873	0.9881	0.9873	1.1147	1.1147	1.1152	1.1147
10	1.0297	1.0297	1.0297	1.0297	1.1791	1.1791	1.1800	1.1791	1.3388	1.3388	1.3394	1.3388
30	1.4873	1.4873	1.4873	1.4873	1.7198	1.7198	1.7210	1.7198	1.9706	1.9706	1.9714	1.9706
60	1.8746	1.8746	1.8746	1.8746	2.1776	2.1776	2.1791	2.1776	2.5054	2.5054	2.5063	2.5054
100	2.2229	2.2229	2.2229	2.2229	2.5892	2.5892	2.5910	2.5892	2.9863	2.9863	2.9874	2.9863

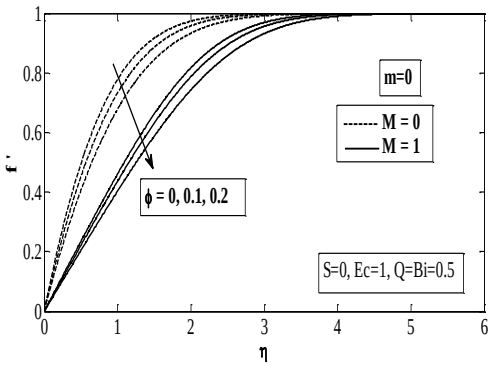

(a)

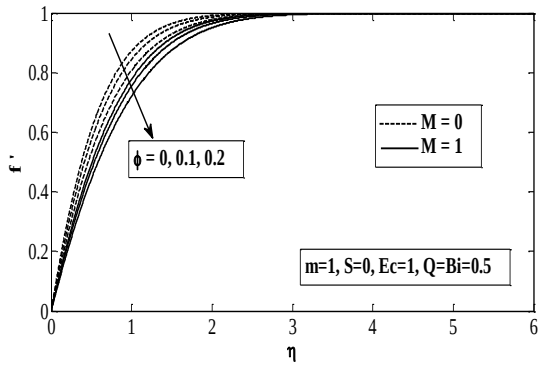

(b)

1. Effect of M on velocity of water-based SWCNTs for (a) flow past horizontal and (b) flow near the stagnation point of vertical stationary flat plates.

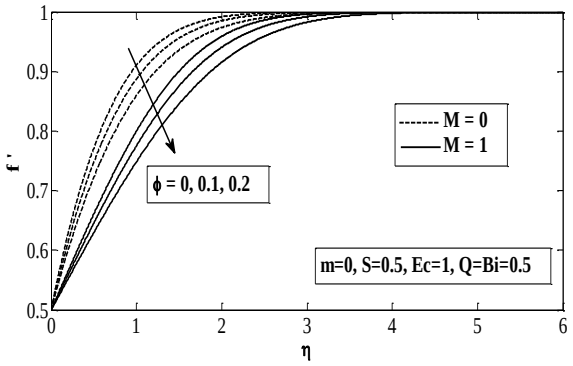

(a)

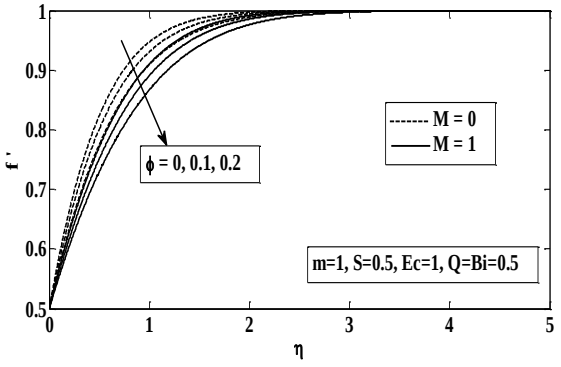

(b)

2 Effect of M on velocity of water-based nanofluids for (a) flow past horizontal and (b) flow near the stagnation point of vertical flat plates moving in the same direction.

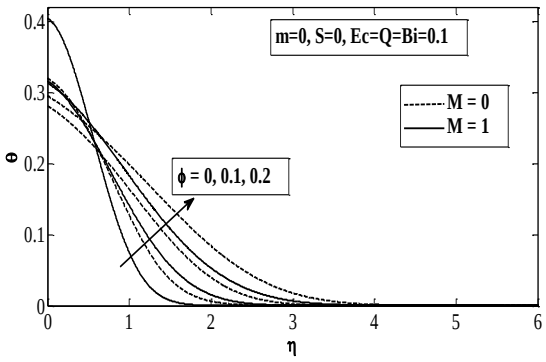

(a)

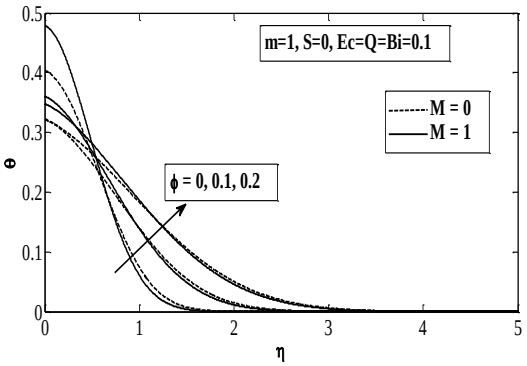

(b)

3. Effect of M on temperature of water-based nanofluids for (a) flow past horizontal and (b) flow near the stagnation point of vertical stationary flat plates.

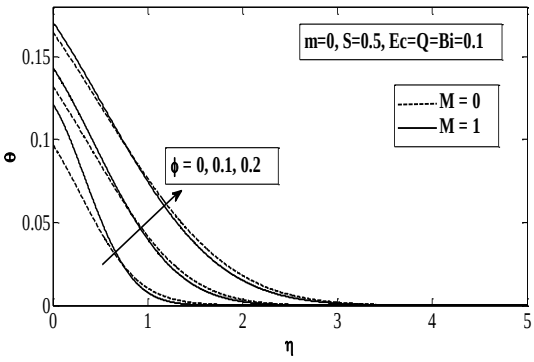

(a)

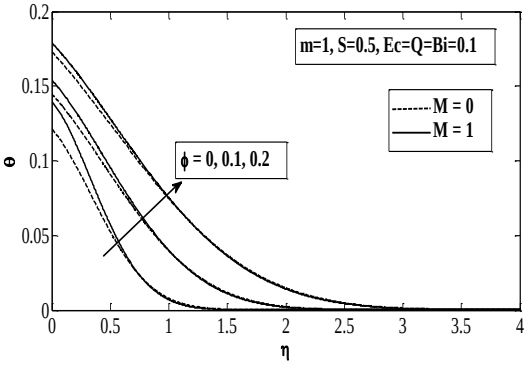

(b)

4. Effect of M on temperature of water-based nanofluids for (a) flow past horizontal and (b) flow near the stagnation point of vertical flat plates moving in the same direction.

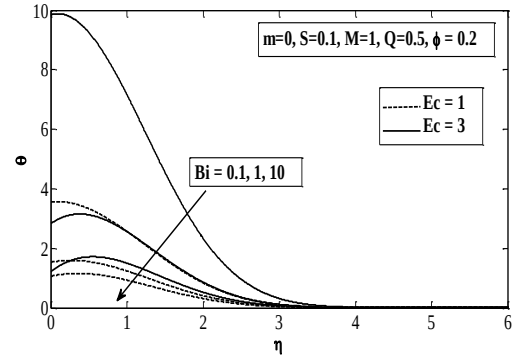

(a)

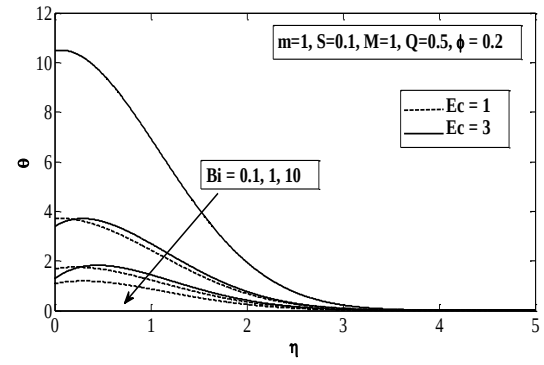

DOI: 10.18535/ijecs/v5i2.22

(b)

5. Effect of Bi on temperature of water-based nanofluids for (a) flow past horizontal and (b) flow near the stagnation point of vertical flat plates moving in the same direction.

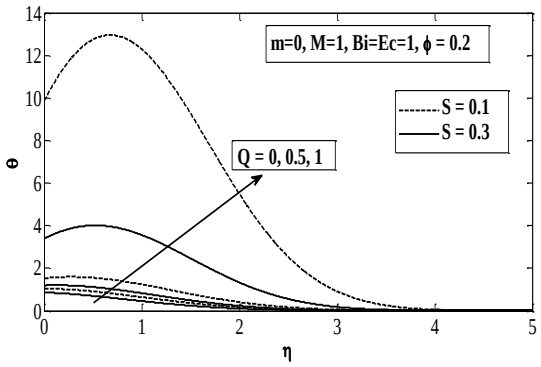

(a)

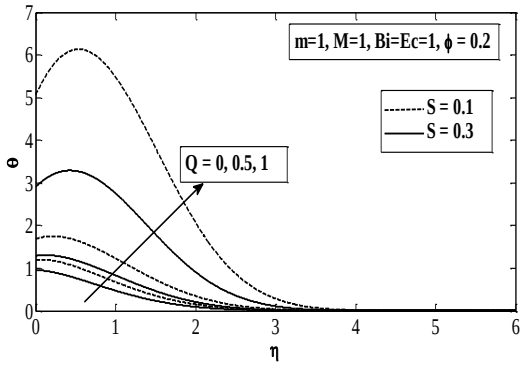

(b)

6. Effect of Q on temperature of water-based nanofluids for (a) flow past horizontal and (b) flow near the stagnation point of vertical flat plates moving in the same direction.

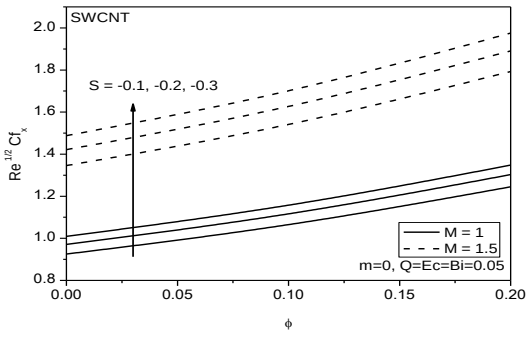

(a)

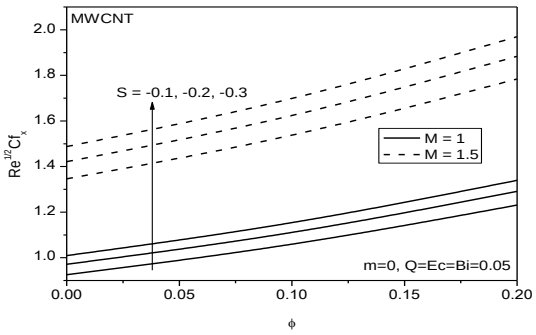

(b)

Figure 7: Variation of skin friction with volume fraction of nanoparticles and magnetic field along a horizontal plate moving in opposite direction to the free stream for (a) SWCNTs and (b) MWCNTs.

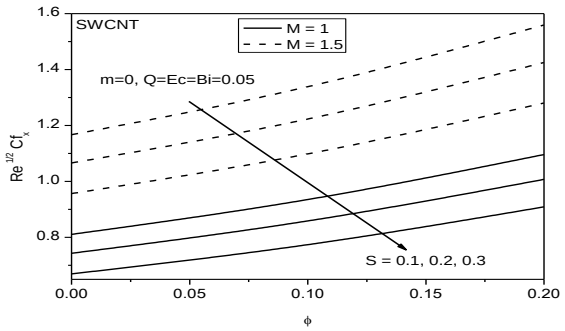

(a)

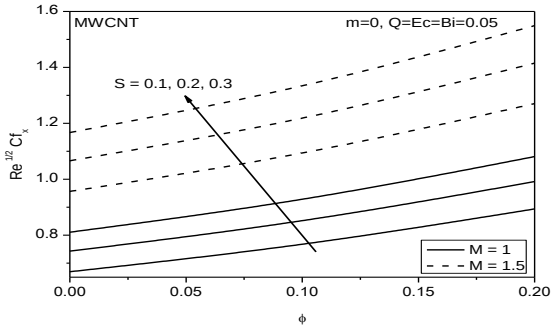

(b)

Figure 8: Variation of skin friction with volume fraction of nanoparticles and magnetic field along a horizontal plate moving in same direction to the free stream for (a) SWCNTs and (b) MWCNTs.

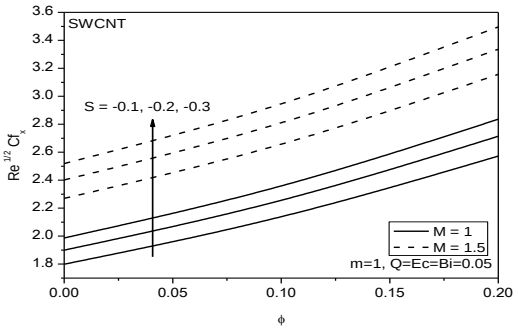

(a)

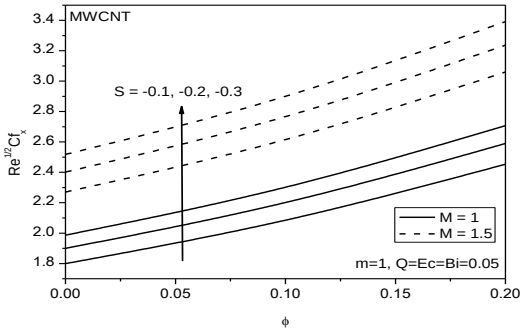

(b)

Figure 9: Variation of skin friction with volume fraction of nanoparticles and magnetic field along a vertical plate moving in opposite direction to the free stream for (a) SWCNTs and (b) MWCNTs.

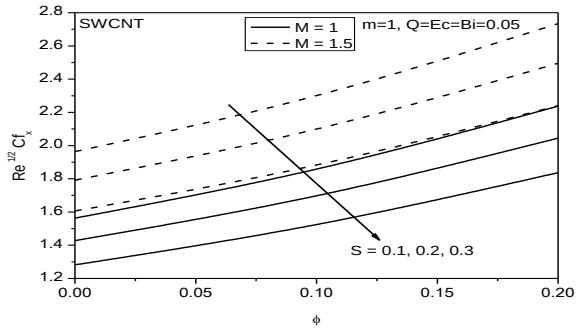

(a)

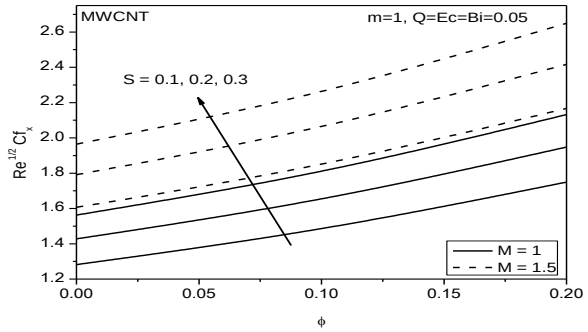

(b)

Figure 10:Variation of skin friction with volume fraction of nanoparticles and magnetic field along a vertical plate moving in same direction to the free stream for (a) SWCNTs and (b) MWCNTs.

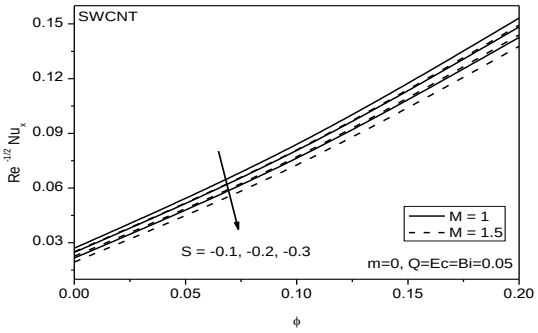

(a)

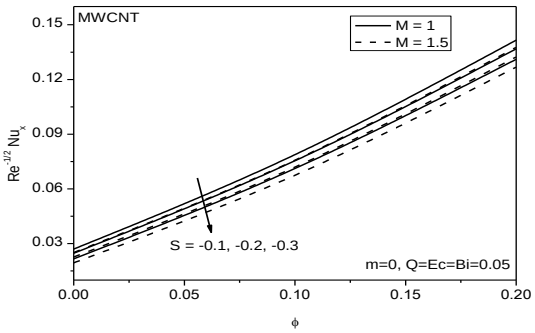

(b)

11. Variation of Nusselt number with volume fraction of nanoparticles and magnetic field along a horizontal plate moving in opposite direction to the free stream for (a) SWCNTs and (b) MWCNTs

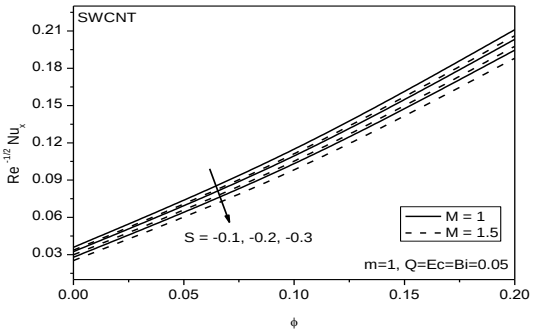

(a)

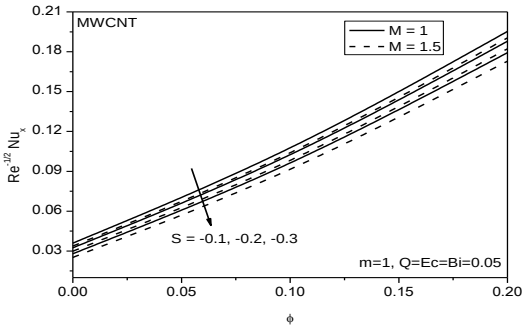

(b)

DOI: 10.18535/ijecs/v5i2.22

12. Variation of Nusselt number with volume fraction of nanoparticles and magnetic field along a vertical plate moving in opposite direction to the free stream for (a) SWCNTs and (b) MWCNTs.

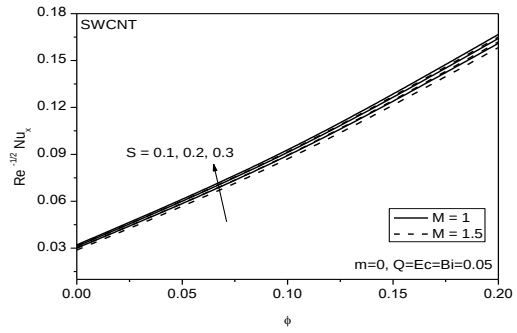

(a)

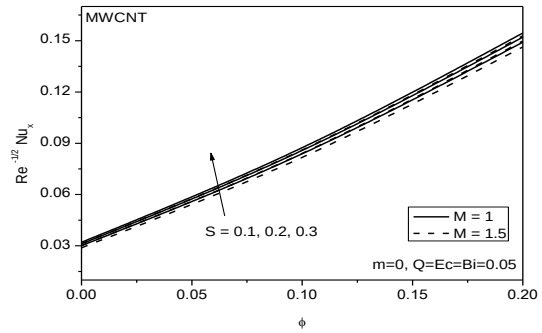

(b)

13. Variation of Nusselt number with volume fraction of nanoparticles and magnetic field along a horizontal plate moving in same direction to the free stream for (a) SWCNTs and (b) MWCNTs.

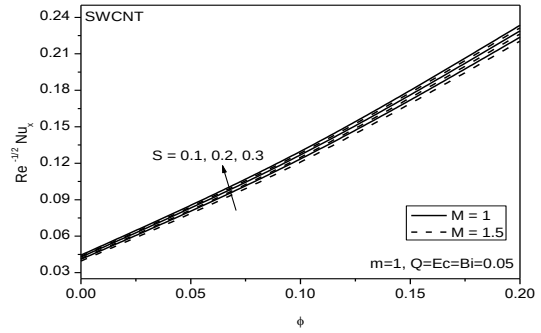

(a)

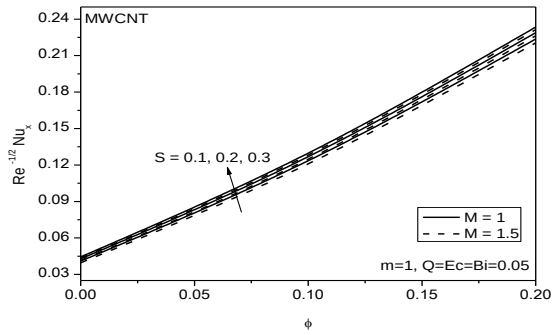

(b)

14. Variation of Nusselt number with volume fraction of nanoparticles and magnetic field along a vertical plate moving in same direction to the free stream for (a) SWCNTs and (b) MWCNTs.

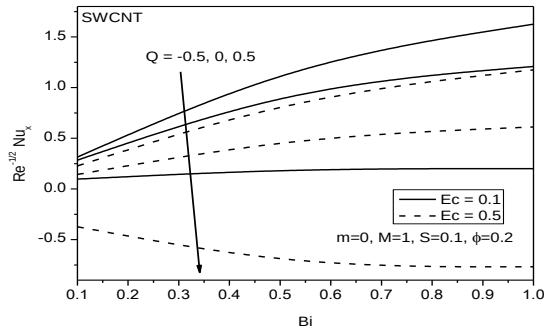

(a)

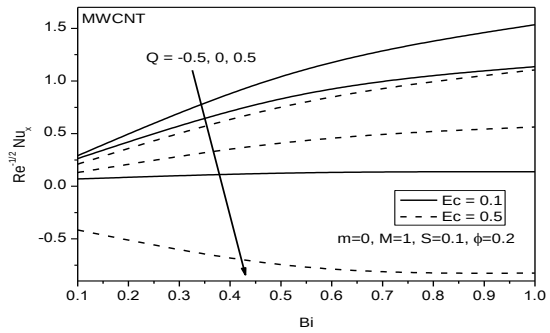

(b)

15. Variation of Nusselt number with convective parameter and Eckert number along a horizontal plate moving in same direction to the free stream for (a) SWCNTs and (b) MWCNTs.

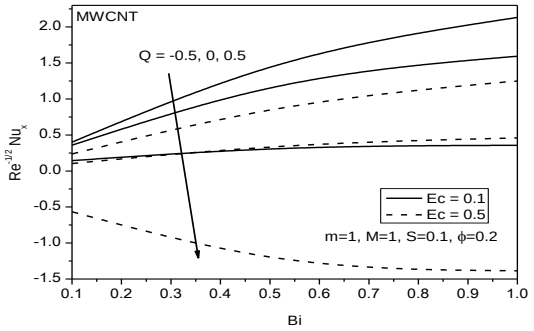

(a)

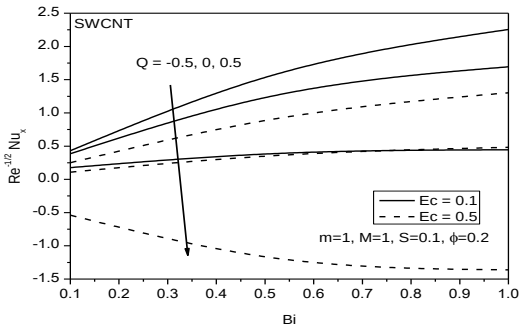

(b)

16. Variation of Nusselt number with convective parameter and Eckert number along a vertical plate moving in same direction to the free stream for (a) SWCNTs and (b) MWCNTs.

References

1. Choi, S.U.S., (1995), Enhancing thermal conductivity of fluid with nanoparticles, developments and applications of non-Newtonian flow. ASME FED, Vol.231, pp.99-105.
2. Masuda, H., Ebata, A., Teramae, K., and Hishinuma, N., (1993), Alteration of thermal conductivity and viscosity of liquid by dispersing ultra-fine particles, Netsu Bussei, Vol.7, pp.227-233.
3. Buongiorno, J., Hu, W., (2005), Nanofluid coolants for advanced nuclear power plants, Proceedings of ICAPP 05: May 2005 Seoul. Sydney: Curran Associates, Inc; pp.15-19.
4. Buongiorno, J., (2006), Convective transport in nanofluids, ASME J Heat Transf, Vol.128, pp.240-250.
5. Kuznetsov, A.V., and Nield, D.A., (2010), Natural convective boundary-layer flow of a nanofluid past a vertical plate, Int J Thermal Sci., Vol.49, pp.243-247.
6. Nield, D.A., and Kuznetsov, A.V., (2009), The Cheng-Minkowycz problem for natural convective boundary-layer flow in a porous medium saturated by a nanofluid, Int J Heat Mass Transf., Vol.52, pp.5792-5795.
7. Nield, D.A., and Kuznetsov, A.V., (2011), The Cheng-Minkowycz problem for the double diffusive natural convective boundary-layer flow in a porous medium saturated by a nanofluid, Int J Heat Mass Transf., Vol.54, pp.374-378.
8. Cheng, P., Minkowycz, W.J., (1977), Free convection about a vertical flat plate embedded in a porous medium with application to heat transfer from a dike, J Geophysics Research, Vol.82, No.14, pp.2040-2044.
9. Hone J., (2004), Carbon nanotubes: thermal properties, Dekker Encycl Nanosci Nanotechnol, pp.603–610
10. Antar Z, Noel H, Feller JF, Glouannec P, Elleuch K., (2012), Thermophysical and radiative properties of conductive biopolymer composite, Mater Sci Forum., Vol.714, pp.115–122.
11. Ding Y., Alias H., Wen D., Williams R.A., (2006), Heat transfer of aqueous suspensions of carbon nanotubes (CNT nanofluids), Int J Heat Mass Transf., Vol.49 (1-2), pp.240–250.
12. Kamali R., Binesh A., (2010), Numerical investigation of heat transfer enhancement using carbon nanotube-based non-Newtonian nanofluids, Int Commun Heat Mass Transf., Vol.37(8):1153–1157
13. Meyer J, McKrell T, Grote K (2013) The influence of multi-walled carbon nanotubes on single-phase heat transfer and pressure drop characteristics in the transitional flow regime of smooth tubes. Int J Heat Mass Transf 58(1-2):597–609.
14. Khan W. A., Khan Z. H., and Rahi M., (2013), Fluid flow and heat transfer of carbon nanotubes along a flat plate with Navier slip boundary, Appl Nanosci., DOI 10.1007/s13204-013-0242-9.
15. Waqar A. Khan, Richard Culham, and Rizwan U Haq, (2015), Heat Transfer Analysis of MHD Water Functionalized Carbon Nanotube Flow over a Static/Moving Wedge, Hindawi Publishing Corporation, Journal of Nanomaterials, Volume 2015, Article ID 934367, 13 pages
16. Van Rij, J., Ameel, T., Harman, T., (2009), The effect of viscous dissipation and rarefaction on rectangular microchannel convective heat transfer. *Int. J. Therm. Sci.* 2009, *48*, 271–281.
17. Koo, J., Kleinstreuer, C., (2004), Viscous dissipation effects in microtubes and microchannels, *Int. J. Heat Mass Transf., Vol. 47*, pp.3159-3169.
18. Mohammad H. Yazdi, Shahrir Abdullah, Ishak Hashim and Kamaruzzaman Sopian, (2011), Effects of Viscous Dissipation on the Slip MHD Flow and Heat Transfer past a Permeable Surface with Convective Boundary Conditions, *Energies*, Vol.*4*, pp.2273-2294.
19. Khan, S.K., Subhas Abel, M., and Sonth Ravi, M., (2003), Viscoelastic MHD flow, heat and mass transfer over a porous stretching sheet with dissipation of energy and stress work, Int J Heat Mass Transf., Vol.40, pp.47-57.
20. Md Shakhaoath Khan, Ifsana Karim, Lasker Ershad Ali and Ariful Islam, (2012), Unsteady MHD free convection boundary-layer flow of a nanofluid along a stretching sheet with thermal radiation and viscous dissipation effects, International Nano Letters, 2:24,pp.1-9.
21. Makinde, O. D., (2012), Analysis of Sakiadis flow of nanofluids with viscous dissipation and

Newtonian heating, Appl. Math. Mech. -Engl. Ed., Vol.33(12), pp.1545-1554.
22. Chandrasekar, M., and Baskaran, S., (2007), Thermodynamical modelling of viscous dissipation in magnetohydrodynamic Flow, Theoret. Appl. Mech., Vol.34, No.3, pp. 197-219.
23. Fekry M Hady, Fouad S Ibrahim, Sahar M Abdel-Gaied and Mohamed R Eid, (2012), Radiation effect on viscous flow of a nanofluid and heat transfer over a nonlinearly stretching sheet, Nanoscale Research Letters, Vol.7:229
24. Hone, J., (2004), "Carbon nanotubes: thermal properties," in Dekker Encyclopedia of Nanoscience and Nanotechnology, pp. 603–610.
25. Ruoff R. S. and Lorents, D. C., (1995), "Mechanical and thermal properties of carbon nanotubes," Carbon, Vol. 33, No. 7, pp. 925–930.
26. Shampine, L. F., and Kierzenka, J., (2000), "Solving boundary value problems for ordinary differential equations in MATLAB with bvp4c," Tutorial Notes.
27. White, F. M., (1991), Viscous Fluid Flow, McGraw-Hill, NewYork, NY, USA, 2nd edition.
28. Yacob, N. A., Ishak, A. and Pop, I., (2011), "Falkner-Skan problem for a static or moving wedge in nanofluids," International Journal of Thermal Sciences, vol. 50, no. 2, pp. 133–139, 2011.
29. Yih, K. A., (1998), "Uniform suction/blowing effect on forced convection about awedge: uniformheat flux," Acta Mechanica, vol. 128, no. 3-4, pp. 173–181, 1998.
30. Khan W. A. and Pop, I., (2013), "Boundary layer flow past a wedge moving in a nanofluid," Mathematical Problems in Engineering, vol. 2013, Article ID 637285, 7 pages.
31. Kuo, B.L.(2005), "Heat transfer analysis for the Falkner-Skan wedge flow by the differential transformation method," International Journal of Heat and Mass Transfer, vol. 48, no. 23-24, pp. 5036– 5046.
32. Rajagopal, K. R., Gupta, A. S. and T. Y. Na, (1983), "A note on the Falkner-Skan flows of a non-Newtonian fluid," International Journal of Non-Linear Mechanics, vol. 18, no. 4, pp. 313–320, 1983.
33. Blasius, H., (1908), "Grenzschichten in Flussigkeiten mit kleiner Reibung," ZentralblattMathematical Physics, vol. 56, pp. 1–37.